Cancer Cell
Article

Identification of miRNomes in Human Liver and Hepatocellular Carcinoma Reveals miR-199a/b-3p as Therapeutic Target for Hepatocellular Carcinoma

Jin Hou,[1,2,11] Li Lin,[3,11] Weiping Zhou,[4,11] Zhengxin Wang,[5] Guoshan Ding,[5] Qiongzhu Dong,[6] Lunxiu Qin,[6] Xiaobing Wu,[7] Yuanyuan Zheng,[1] Yun Yang,[4] Wei Tian,[8] Qian Zhang,[1] Chunmei Wang,[1] Qinghua Zhang,[1] Shi-Mei Zhuang,[9] Limin Zheng,[9] Anmin Liang,[10] Wenzhao Tao,[1] and Xuetao Cao[1,2,*]

[1]National Key Laboratory of Medical Immunology & Institute of Immunology, Second Military Medical University, Shanghai 200433, China
[2]Institute of Immunology, Tsinghua University School of Medicine, Beijing 100084, China
[3]Institute of Immunology, Zhejiang University School of Medicine, Hangzhou 310058, China
[4]Third Department of Hepatic Surgery, Eastern Hepatobiliary Surgery Hospital, Shanghai 200438, China
[5]Department of Organ Transplantation, Shanghai Changzheng Hospital, Shanghai 200003, China
[6]Liver Cancer Institute and Zhongshan Hospital, Institutes of Biomedical Science, Fudan University, Shanghai 200032, China
[7]National Lab of Molecular Virology and Genetic Engineering, Beijing 100052, China
[8]Beijing Genomics Institute, Shenzhen 518083, China
[9]School of Life Sciences, Sun Yat-sen University, Guangzhou 510275, China
[10]Affiliated Tumor Hospital of Guangxi Medical University, Nanning 530021, China
[11]These authors contributed equally to this work
*Correspondence: caoxt@immunol.org
DOI 10.1016/j.ccr.2011.01.001

SUMMARY

The full scale of human miRNome in specific cell or tissue, especially in cancers, remains to be determined. An in-depth analysis of miRNomes in human normal liver, hepatitis liver, and hepatocellular carcinoma (HCC) was carried out in this study. We found nine miRNAs accounted for ~88.2% of the miRNome in human liver. The third most highly expressed miR-199a/b-3p is consistently decreased in HCC, and its decrement significantly correlates with poor survival of HCC patients. Moreover, miR-199a/b-3p can target tumor-promoting PAK4 to suppress HCC growth through inhibiting PAK4/Raf/MEK/ERK pathway both in vitro and in vivo. Our study provides miRNomes of human liver and HCC and contributes to better understanding of the important deregulated miRNAs in HCC and liver diseases.

INTRODUCTION

MicroRNAs (miRNAs) inhibit translation or induce mRNA degradation in general by binding to the 3′ untranslational region (3′ UTR) of target mRNAs. Since initial observation, about 1000 human miRNAs have been registered in miRBase (v.14.0) (Griffiths-Jones et al., 2006). Although a previous classical approach of cloning has partially revealed miRNA expression profile in a panel of mammalian tissues and cell types (Landgraf et al., 2007; Basso et al., 2009), low throughput with low sensitivity and poor resolution makes these approaches unlikely to define miRNome. Massively parallel signature sequencing (MPSS) of miRNAs can identify miRNome in-depth, which reveals miRNA expression differences as well as the individual miRNA abundance. As a minimum threshold amount must be reached for miRNAs to repress target mRNAs (Brown et al., 2007; Sarasin-Filipowicz et al., 2009), the abundance of miRNAs and their ratios in the entire miRNome of specific cell or tissue may be more important for their functions.

Infection of hepatitis B Virus (HBV) or hepatitis C Virus (HCV) in human liver induces the development of chronic hepatitis, liver cirrhosis, and in some instances hepatocellular carcinoma (HCC). HCC is among the leading causes of cancer-related deaths in Asia, especially in China. Previous reports suggested

Significance

The full-scale analysis of miRNomes in human normal liver, hepatitis liver, and HCC led us to conclude that miR-199a/b-3p, the third most abundant miRNA in the liver, might be an important deregulated miRNA in HCC. Low miR-199a/b-3p expression strongly correlates with the markedly reduced survival of HCC patients. AAV8-mediated in vivo gene delivery in the subcutaneous and orthotopic human HCC-bearing mouse models demonstrate miR-199a/b-3p's therapeutic potential. The miRNomes of human normal liver, hepatitis liver, and HCC may present a resource for researching the roles of miRNAs in liver biology and liver diseases.

Table 1. Most Abundantly Expressed miRNAs in Human Normal Liver

miRNA	TPM in Normal Liver Sample 1	TPM in Normal Liver Sample 2	TPM in Normal Liver Sample 3	Average TPM in Normal Liver	Average Ratio in miRNome
miR-122	529,834	508,274	522,504	520,204	52.0%
miR-192	176,591	170,585	160,383	169,186	16.9%
miR-199a/b-3p	45,033	49,702	51,920	48,885	4.9%
miR-101	33,431	37,296	39,285	36,671	3.7%
let-7a	29,899	34,474	33,908	32,760	3.3%
miR-99a	22,430	22,756	20,583	21,923	2.2%
let-7c	18,848	21,356	23,870	21,358	2.1%
let-7b	16,255	19,960	13,938	16,718	1.7%
let-7f	13,786	13,888	16,598	14,757	1.5%
Total	886,107	878,291	882,989	882,462	88.2%

TPM, transcripts per million. See also Table S1.

some deregulated miRNAs in HCC but none of them was based on deep sequencing (Gramantieri et al., 2007, 2008, 2009; Braconi and Patel, 2008; Ji et al., 2009a, 2009b; Ladeiro et al., 2008; Varnholt et al., 2008; Wang et al., 2008, 2009a; Wong et al., 2008; Murakami et al., 2006; Kutay et al., 2006; Budhu et al., 2008; Ura et al., 2009; Coulouarn et al., 2009; Xiong et al., 2010). The abundance of these deregulated miRNAs remains unknown to date. The results obtained from only microarray or real-time quantitative RT-PCR (qRT-PCR) might be controversial and complicated. Therefore, identification of miRNomes in human normal liver tissue, HBV or HCV-infected liver tissues and HCC in-depth may reveal the important deregulated miRNAs in HCC.

RESULTS

miRNomes in Human Normal Liver, Hepatitis Liver, and HCC

We applied MPSS to carry out an in-depth analysis of the miRNomes in three normal liver tissues (distal normal liver tissue of liver hemangioma), an HBV-infected liver, a severe chronic hepatitis B liver, two HBV-related HCCs, an HCV-related HCC, and an HCC without HBV or HCV infection. Clean sequenced reads were used for further analysis (see Experimental Procedures; see Table S1 available online). The abundance value of each known miRNA was normalized using "transcripts per million (TPM)" in each small RNA library. Except for HCC, the known miRNAs exhibited a similar distribution in each library based on classification of TPM degrees. In normal liver tissue, ~85.9% miRNAs were poorly expressed (<10 TPM), ~13.2% miRNAs were expressed modestly (10–10,000 TPM), and only ~0.9% (9) miRNAs were expressed abundantly (>10,000 TPM) but they accounted for ~88.2% of all miRNA reads (Table 1). The three most abundantly expressed miRNAs were miR-122, miR-192, and miR-199a/b-3p, accounting for ~52.0%, ~16.9%, and ~4.9% of the miRNome, respectively.

Deregulated Abundant miRNAs in HCC

Which miRNA, especially those unreported before, is the major player in HCC pathogenesis? As only a few miRNAs are abundantly expressed in the miRNome and they seem to be the most important in liver biology and HCC, only miRNAs with TPM >2000 (accounting for ~99% of the miRNome) and more than 1-fold alteration were considered most likely to be important in HCC pathogenesis in this study (Table 2; Tables S2 and S3). miR-199a/b-3p was markedly decreased in all the sequenced HCC samples as compared with matched nonneoplastic liver tissues. We also sequenced different regions of nonneoplastic liver tissues to confirm their reliability and found their miRNomes similar (Table S2).

The deregulated abundant miRNAs in HCC were further confirmed by qRT-PCR in 40 HBV-related HCC, five HCV-related HCC, and three HCC of other etiologies (Table S4). The ratio of HCC samples with more than 1-fold increment or decrement of the individual miRNA was shown in Table 3 and Table S5. Among these abundant miRNAs, miR-199a/b-3p expression was the most consistently and markedly decreased. However, many previously reported deregulated miRNAs in HCC were found to be expressed at relatively low levels which might make them less important in HCC pathogenesis (Table S6), and some of them seemed unchanged in the sequencing data. Also, expression of abundant miR-122 and let-7 members were less consistently decreased in HCC samples (Table 3). Interestingly, no significant difference between miRNomes of HBV or HCV-infected liver tissues and normal liver tissue was found (Table 2; Table S2). Additionally, some miRNAs, poorly expressed but markedly altered in the sequenced HCC samples, were confirmed by qRT-PCR, and they were also less consistently deregulated (Table S7). Together, the miRNomes of human normal liver, hepatitis liver and HCC led us to identify the consistently deregulated miRNA in HCC.

To further investigate whether the deregulated abundant miRNAs correlate with the survival of HCC patients, we investigated two independent cohorts of HCC patients, Cohort 1 of 142 patients and Cohort 2 of 152 patients (Table S8). As compared with the matched nonneoplastic tissue of each HCC sample, miR-199a/b-3p level decreased in ~88% (125/142, Cohort 1) and ~86% (130/152, Cohort 2) of the HCC samples while miR-122 level decreased in ~46% (66/142, Cohort 1) and ~47% (72/152, Cohort 2) of them. Kaplan-Meier analysis revealed that low miR-199a/b-3p level in HCC tissues significantly correlated with the markedly reduced tumor-free survival and overall survival of HCC patients (Figure 1), suggesting the important roles of miR-199a/b-3p in pathogenesis of HCC and

Table 2. Most Abundantly Expressed miRNAs in HCC and Matched Nonneoplastic Liver Tissues

miRNA	Average in Normal Liver	HBV(+) Adjacent Sample 1	HBV(+) HCC Sample 1	HBV(+) Adjacent Sample 2	HBV(+) HCC Sample 2	HCV(+) Adjacent	HCV(+) HCC	HBV(-) HCV(-) Adjacent Tissue	HBV(-) HCV(-) HCC
miR-122[a]	520,204	497,436	581,733	478,691	516,360	449,921	511,457	597,746	17,280
miR-192[a]	169,186	184,230	182,858	153,346	205,819	111,731	166,201	111,530	164,532
199a/b-3p[b]	48,885	79,099	2588	58,199	2211	44,000	2831	39,779	2979
miR-101[a]	36,671	37,538	35,730	54,202	44,686	26,361	38,555	57,519	39,321
let-7a [b]	32,760	26,392	5515	39,339	40,747	36,908	28,419	26,423	110,611
miR-99a[b]	21,923	22,139	6019	27,594	10,326	20,701	6107	18,287	984
let-7c[b]	21,358	20,724	2930	19,340	15,231	18,996	17,059	19,840	1902
let-7b[b]	16,718	20,556	1531	11,819	2951	20,767	8864	12,944	19,074
let-7f [a]	14,757	12,778	10,047	14,195	12,139	14,230	14,552	19,600	133,023
let-7d[b]	8792	5326	1264	8605	6390	9110	6471	6256	56,226
miR-100[b]	3606	4166	81	5959	7863	4763	7708	2742	998
125b-5p[b]	2665	2043	234	2634	992	1542	1391	1368	76
miR-143[b]	2269	2254	750	2635	996	6167	763	1278	4573
miR-29c[b]	2009	2067	670	2189	1062	3012	2301	3059	2266
miR-21[c]	5465	9561	16,241	10,099	12,314	9133	9356	10,948	82,662
miR-146b[c]	1614	698	7817	602	171	2737	643	597	555
miR-92a[c]	955	4775	16,142	874	420	2009	1650	1370	4269

Expressions of the abundant miRNAs seem.
[a] unaltered.
[b] decreased.
[c] increased in HCC. See also Tables S2 and S3.

prognosis of HCC patients. However, low miR-122 or let-7 member expression in HCC tissues did not seem to significantly correlate with the survival of HCC patients (Figure S1). Furthermore, in two other independent cohorts of HCC patients, Cohort 3 and Cohort 4, we validated that low miR-199a/b-3p level significantly correlated with the markedly reduced tumor-free survival of HCC patients, but low miR-122 or let-7 member level did not (Figure S1). Additionally, we performed Cox proportional hazards regression analysis to exclude the confounder effect. Univariate analysis was performed to identify factors which might affect the tumor-free survival of HCC patients, followed by multivariate analysis, which is controlled for potential confounders. Significantly, in all the four independent HCC cohorts, multivariate analysis confirmed that low miR-199a/b-3p expression was an independent predictor for reduced tumor-free survival of HCC patients (Table S9). Thus, these results indicate the importance of miR-199a/b-3p expression in human liver and HCC.

Deregulated Histone Methylation Mediates Decrease of miR-199a/b-3p Expression

As miR-199a/b-3p was found to be the consistently and markedly decreased miRNA in HCC, we investigated the underlying mechanism for the repression of miR-199a/b-3p in eight additional HCC samples (Table S10) in which miR-199a/b-3p level decreased over 90% as compared with matched controls (data not shown). miR-199a/b-3p is expressed from three precursors in human genome: miR-199a-1 (Chromosome 19), miR-199a-2 (Chromosome 1), and miR-199b (Chromosome 9), sharing the same 3p mature miRNA. We first identified that miR-199a/b-3p is mainly expressed from miR-199a-2 by detecting its precursors (Figure 2A; Figure S2A), and pri-miR-199a-2 expression is markedly decreased in HCC (Figure 2B), but pri-miR-199b expression is not altered (data not shown). Second, we ruled out the possibility that the three miR-199 genes were deleted in HCC genome, as equal amounts of them were detected in equal amounts of genomic DNA extracted from HCC and matched controls using real-time PCR (data not shown). Third, in the reported CpG islands known to regulate miR-199a-1 and -2 expression (Kim et al., 2008), we found these regions hypermethylated in both HCC and matched controls through bisulfate sequencing (Figure S2B), thus indicating DNA methylation is less likely to regulate their expression in the liver. Fourth, as methylation of histone H3 at Lys4 (H3K4) is linked to transcriptional activation, while methylation of H3 at K9 or K27 and of H4 at K20 is linked to transcriptional repression (Esteller, 2008), reported genomic regulatory regions (Kim et al., 2008) (Figure 2C) of miR-199a-1 and -2 in HCC showed a reduced level of H3K4 trimethylation (H3K4me3) but increased H3K9me3 and H3K27me3 (Figure 2D), and the level of H4K20me3 was almost equal to that of matched controls (data not shown). These results indicate that reduced expression of miR-199a/b-3p in HCC is mediated by histone modification and independent of DNA methylation.

miR-199a/b-3p Inhibits HCC Growth

We then investigated the pathophysiological significance, and its underlying mechanisms, of the silenced miR-199a/b-3p in HCC.

Table 3. Confirmation of Deregulated miRNAs in 40 HBV-Related HCC Samples Compared with Matched Controls Using qRT-PCR

	Samples of Increased miRNA Expression		Samples of Decreased miRNA Expression	
miRNA	Ratio of Increased Samples	Average HCC/Control in Increased Samples	Ratio of Decreased Samples	Average HCC/Control in Decreased Samples
miR-122	—	—	18/40 (45%)	0.34 ± 0.09
miR-192	2/40 (5%)	2.57 ± 0.58	1/40 (3%)	0.39
miR-199a/b-3p	—	—	40/40 (100%)	0.12 ± 0.11
miR-99a	—	—	34/40 (85%)	0.15 ± 0.12
miR-125b-5p	—	—	33/40 (83%)	0.15 ± 0.12
miR-100	—	—	31/40 (78%)	0.14 ± 0.11
miR-29c	—	—	28/40 (70%)	0.30 ± 0.10
miR-143	—	—	26/40 (65%)	0.23 ± 0.13
let-7a	—	—	6/40 (15%)	0.36 ± 0.07
let-7b	—	—	13/40 (33%)	0.26 ± 0.11
let-7c	—	—	4/40 (10%)	0.36 ± 0.14
let-7d	—	—	3/40 (8%)	0.40 ± 0.12
miR-21	20/40 (50%)	4.76 ± 2.62	5/40 (13%)	0.41 ± 0.05
miR-92a	7/40 (18%)	3.07 ± 1.02	4/40 (10%)	0.37 ± 0.04
miR-146b	6/40 (15%)	12.9 ± 8.9	12/40 (30%)	0.31 ± 0.11

Data of HCC/control are shown as mean ± SD (n = samples with deregulated miRNA expression). See also Tables S4–S7.

The silencing of miR-199a/b-3p prompted us to investigate whether miR-199a/b-3p functions as a tumor suppressor in HCC. In HCC cell lines Hep3B, SMMC-7721, Huh7, and HepG2, miR-199a/b-3p expression was markedly decreased compared with that in human normal liver (Figure 3A; Figure S3A), and transfection of miR-199a/b-3p restored its expression in these cells (Figure 3B; Figure S3B). Restoration of miR-199a/b-3p expression in HCC cell lines repressed cell growth (Figure 3C; Figure S3C), induced cell apoptosis (Figure 3D), and inhibited cell cycle progression, which might be G1-phase arrest (Figure 3E). Additionally, in miR-199a/b-3p stably overexpressed Hep3B and SMMC-7721 cells, cell growth rate was also significantly decreased compared with the control cells (Figures 3F and 3G). These results demonstrate that miR-199a/b-3p may function as a tumor suppressor in vitro.

In order to investigate the antitumor effect of miR-199a/b-3p in vivo, we prepared a human HCC-bearing mouse model SMMC-LTNM by transplanting histologically intact fresh human HCC tissues to form subcutaneous transplantation tumor in nude mice and then continuously maintained with subcutaneous passage (Tao et al., 1998, 2007). The miRNA expression profile of SMMC-LTNM tumor tissue is similar to that of freshly isolated human HCC tissues, exhibiting equal expression of miR-122 and miR-192 while silenced expression of miR-199a/b-3p as compared with nonneoplastic human liver tissues (Figure 4A). By intratumoral injection of cholesterol-conjugated miR-199a/b-3p mimics (Wolfrum et al., 2007), we found that miR-199a/b-3p expression in tumor was elevated (Figure 4A) while tumor growth was inhibited, serum AFP was reduced, and more significant tumor necrosis was observed (Figures 4B and 4C). Thus, we conclude that restoration of miR-199a/b-3p expression in HCC resulted in dramatic repression of HCC growth.

In order to make the in vivo delivery of miR-199a/b-3p more practical to target HCC, we constructed an adeno-associated virus (AAV) 8 vector system encoding miR-199a/b-3p (AAV8-miR-199a/b-3p) since AAV vectors have been suggested to be promising for therapeutic gene delivery, particularly AAV8 for liver-targeted gene therapy (McCarty, 2008; Kota et al., 2009). Then, we evaluated the therapeutic potential of AAV8-mediated gene delivery of miR-199a/b-3p in human HCC-bearing nude mouse model SMMC-LTNM. Intratumoral injection of AAV8-miR-199a/b-3p in SMMC-LTNM subcutaneous model elevated miR-199a/b-3p expression in tumor (Figure 4D) while inhibited tumor growth, reduced serum AFP, and caused more significant tumor necrosis (Figures 4E and 4F). Importantly, miR-199a/b-3p level was still higher in the liver of wild-type mice 2 months after a single tail vein injection of 1×10^{12} vector genomes (vg) AAV8-miR-199a/b-3p (Figure S4A). And in vivo administration of AAV8-miR-199a/b-3p in wild-type mice did not seem to cause side effects, as demonstrated by normal levels of endogenously expressed abundant miRNAs in transduced liver (Figure S4B); absence of any acute inflammation, fibrosis, or overt histological evidence of toxicity (Figure S4C); and normal levels of serum markers of liver function, such as ALT and AST (data not shown). Most importantly, in SMMC-LTNM orthotopic model, miR-199a/b-3p expression in tumor was also elevated while tumor growth was inhibited and serum AFP was reduced upon a single tail vein injection of 1×10^{12} vg AAV8-miR-199a/b-3p (Figures 4G and 4H; Figure S4D). These data demonstrate that AAV8 vector system provides an effective, nontoxic mean to deliver miRNAs to the liver or HCC tissue, and in vivo administration of AAV8-miR-199a/b-3p may have considerable potential for HCC gene therapy.

miR-199a/b-3p Targets PAK4

As miRNAs function mainly through inhibition of target genes, the target of miR-199a/b-3p that functions in HCC pathogenesis was further analyzed. The hundreds of predicted target genes in TargetScan (http://www.targetscan.org) were subjected to

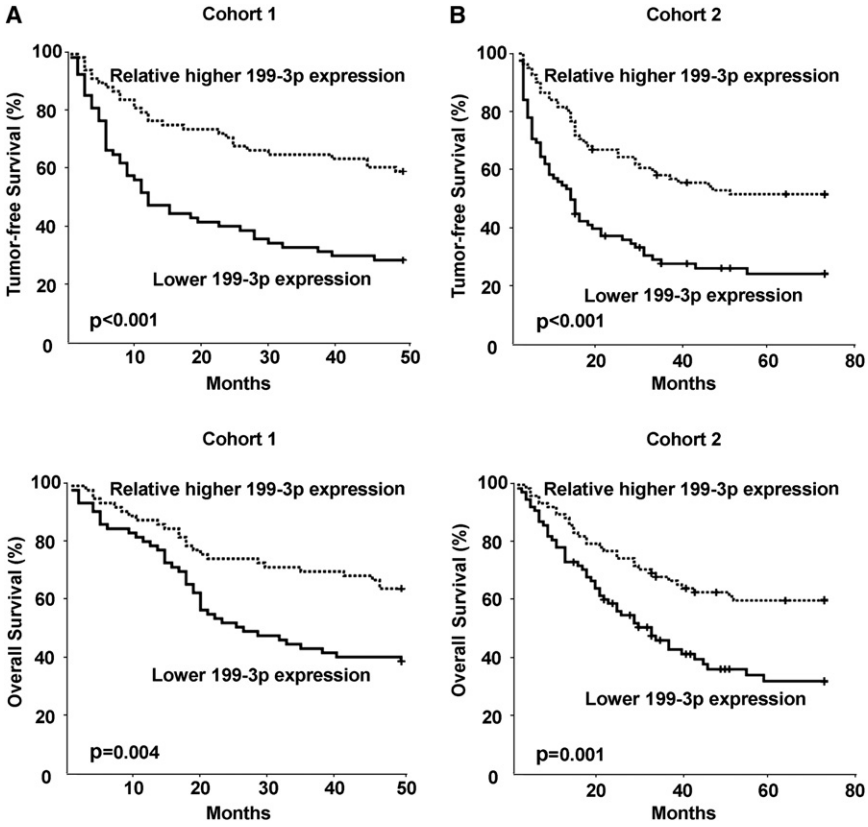

Figure 1. Low miR-199a/b-3p Expression Correlates with Poor Survival of HCC Patients

Shown are Kaplan-Meier survival curves of tumor-free survival and overall survival in Cohort 1 (A) and Cohort 2 (B) according to the ratio of miR-199a/b-3p level in each tumor sample compared with its matched nonneoplastic control, the median value of this ratio in each cohort was chosen as the cutoff point.

See also Figure S1, Tables S8, and S9.

enrichment analysis of cell signaling pathways using Kyoto Encyclopedia of Genes and Genomes (KEGG) pathway database (http://www.genome.jp/kegg/) (Hua et al., 2009). We found that Mitogen-activated protein kinase (MAPK) signaling pathway was the most significantly enriched by the predicted targets of miR-199a/b-3p ($p = 1.66$ E-15) (Table S11 and Figure S5A). By evaluating MAPK activation in miR-199a/b-3p overexpressed HCC Hep3B cells, we found that extracellular signal-regulated kinase (ERK) phosphorylation was inhibited (Figure 5A), while p38 and c-Jun N-terminal kinase (JNK) phosphorylation were not affected (data not shown). In the predicted targets participating in ERK activation, only PAK4, which is overexpressed in various cancer cell lines but its contribution in HCC remains elusive (Eswaran et al., 2009), contains two putative miR-199a/b-3p target sites (Figure S5B). We found that expression of a luciferase reporter containing 3′ UTR of PAK4 was inhibited by cotransfection with miR-199a/b-3p mimics (Figure 5B). Furthermore, PAK4 protein expression was decreased by transfection of miR-199a/b-3p mimics but increased by miR-199a/b-3p inhibitors in Hep3B cells (Figures 5A and 5C). However, PAK4 mRNA level was not significantly influenced by overexpression or inhibition of miR-199a/b-3p (data not shown), suggesting that PAK4 expression could be inhibited by miR-199a/b-3p mainly through translational inhibition. In available HCC protein samples, we confirmed that PAK4 protein level was also increased (Figure 5D), and PAK4 mRNA level was not significantly altered (data not shown), further suggesting a posttranscriptional regulation of PAK4 in HCC. Together, these results prove that endogenous PAK4 is targeted and regulated by miR-199a/b-3p.

To identify the role of PAK4 in HCC pathogenesis, we determined whether inhibition of PAK4, just like miR-199a/b-3p restoration, also resulted in HCC repression. In HCC Hep3B and SMMC-7721 cells, in vitro knockdown of PAK4 repressed cell growth (Figure 5E; Figure S5C), induced cell apoptosis (Figure 5F; Figure S5C), and inhibited cell cycle progression (Figure 5G; Figure S5C). Furthermore, in the SMMC-LTNM model, intratumoral injection of cholesterol-conjugated PAK4 siRNA inhibited PAK4 expression (Figure 5A), suppressed tumor growth, and reduced serum AFP (Figure 5H). Additionally, in PAK4 stably overexpressed Hep3B cells, which transcribed PAK4 mRNA without its 3′ UTR, the induction of cell apoptosis by miR-199a/b-3p restoration decreased as compared with that in control cells (Figure 5I). These data confirm that the antitumor effect of miR-199a/b-3p is mediated by inhibiting its target PAK4.

miR-199a/b-3p Inhibits PAK4/Raf/MEK/ERK Pathway in HCC

PAK4 was known to directly phosphorylate and activate Raf1 (Cammarano et al., 2005), and signaling through the Raf/MEK/ERK cascade is well accepted to play critical prosurvival roles in HCC development (Liu et al., 2006). Therefore, we investigated whether Raf/MEK/ERK pathway was involved in the antitumor effect of miR-199a/b-3p by targeting PAK4. We found that overexpression of miR-199a/b-3p or knockdown of PAK4 inhibited the activation of Raf/MEK/ERK cascade in HCC both in vivo and in vitro (Figure 5A; Figure S5D). Moreover, inhibition of miR-199a/b-3p or overexpression of PAK4 also enhanced the activation of Raf/MEK/ERK pathway in Hep3B cells (Figure 5C). Thus, miR-199a/b-3p can inhibit PAK4/Raf/MEK/ERK pathway to suppress HCC pathogenesis. Importantly, as a single miRNA is likely to target multiple mRNAs (Selbach et al., 2008), miR-199a/b-3p has also been shown to target c-Met downstream signals and PI3K-mTOR pathway (Kim et al., 2008; Fornari et al., 2010). In HCC, c-Met and mTOR expression were also inhibited upon miR-199a/b-3p restoration (Figure S5E). These pathways, well defined to participate in HCC

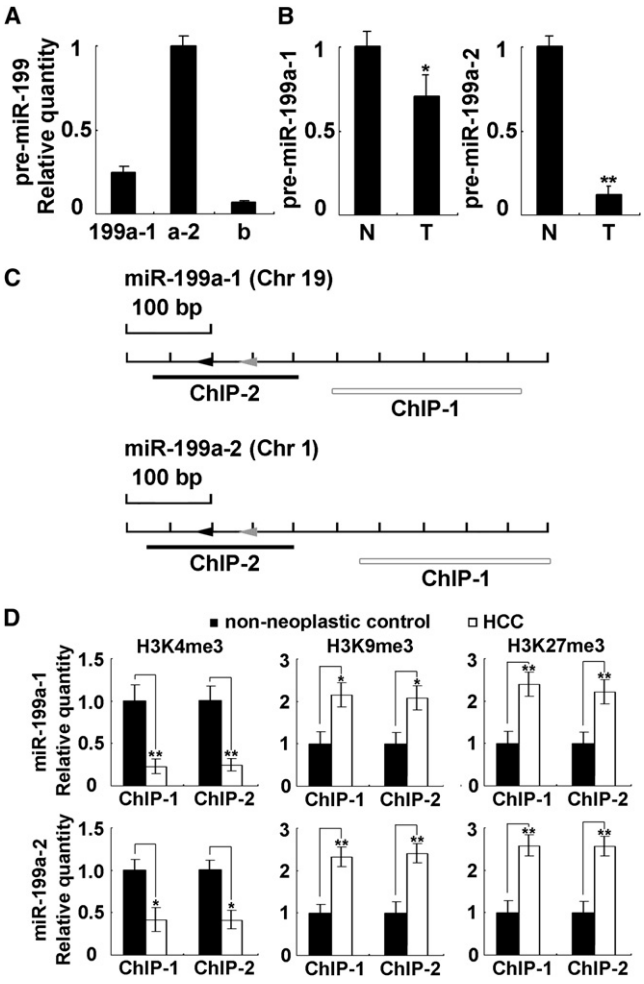

Figure 2. Histone Modifications Mediate Downregulation of miR-199a/b-3p Expression in HCC

(A) Pri-miR-199a-1, pri-miR-199a-2, and pri-miR-199b expression were detected by qRT-PCR in nonneoplastic liver tissues. Data are shown as mean ± SD (n = 8). *, $p < 0.05$; **, $p < 0.01$.

(B) Pri-miR-199a-1 and pri-miR-199a-2 expressions were detected by qRT-PCR in eight HCC samples and matched controls. Data are shown as in (A). N, matched nonneoplastic control; T, HCC tissue.

(C) A schematic diagram shows the genomic context of miR-199a-1 and miR-199a-2. Black and gray arrowheads represent miR-199a-3p and miR-199a-5p, respectively. ChIP analysis for H3K4me3, H3K9me3, H3K27me3, and H4K20me3 was done with two sets of primers spanning the reported genomic regulatory regions (shown as filled and open bars).

(D) Real-time PCR analysis of H3K4me3, H3K9me3, and H3K27me3 at the regulatory regions of miR-199a-1 and miR-199a-2 by ChIP assay in eight HCC samples and matched controls. The primers are indicated in (C). Data are shown as in (A).

See also Figure S2 and Table S10.

development, may also contribute to the antitumor effect of miR-199a/b-3p in HCC progression.

DISCUSSION

In order to elucidate the deregulated miRNAs in cancer, several methods, including microarray and qRT-PCR techniques, have been widely used in qualitative miRNA studies. These approaches mainly focus on the alteration of individual miRNA but lack vigor in revealing the abundance of each miRNA in the background of the entire miRNome. Through these approaches, a set of deregulated miRNAs have been revealed in HCC. As miRNAs function mainly through repressing their targets expression, a minimum threshold amount must be reached for miRNAs to exert their function (Brown et al., 2007; Sarasin-Filipowicz et al., 2009). Thus, the abundantly expressed miRNAs seem to be more important than those expressed at relatively low levels. In-depth analysis of miRNome can reveal the expression level of individual miRNA, especially its proportion in the entire miRNome. Based on this approach, we found that only a few miRNAs were abundantly expressed in human normal liver, but they account for a large part of the miRNome. We do not exclude the possibility that the poorly expressed miRNAs may also participate in liver biology, but the abundant ones seem to be prominent more obviously. For miR-122, the most abundant miRNA in human liver, previous reports have shown its antitumor effect in HCC (Kutay et al., 2006; Gramantieri et al., 2007; Coulouarn et al., 2009). However, miR-122 expression was found to be only decreased in about half of the HCC tissues and less relevant to the survival of HCC patients in this study. Hence, the roles of miR-122 in HCC carcinogenesis and progression still need to be further evaluated, especially in the patients with miR-122 decrement. For miR-192, the second most abundant miRNA in human liver, its roles in liver biology and the pathogenesis of liver diseases remain unknown. As to its expression level in HCC, miR-192 does not seem to be significantly deregulated in the HCC samples as we tested here. In contrast to miR-122 and miR-192, miR-199a/b-3p, the third most abundant miRNA in human liver, is decreased in a large part of HCC tissue samples, thus providing clues for the future study of its roles in HCC.

Identifying the molecular markers correlating with the survival of cancer patients attracts much attention. For HCC, deregulated expression of both coding genes and miRNAs has been suggested to have considerable potential in predicting the prognosis of HCC patients (Ji et al., 2009a). Here, miR-199a/b-3p is verified to be frequently decreased in HCC tissues, and its decrement significantly correlates with the survival of HCC patients, outlining a potential marker for predicting the prognosis of HCC patients. Previous reports showed that deregulated miR-26 and miR-29 expression in HCC tissues also correlated with the survival of HCC patients (Ji et al., 2009a; Xiong et al., 2010). Detecting the expression level of these miRNAs, in combination with miR-199a/b-3p and even other coding genes, may be valuable to predict the prognosis of HCC patients more accurately. Additionally, as several other miRNAs, such as miR-99a, miR-125b-5p, miR-100, and miR-143, are also suggested to be deregulated in HCC tissues in this study, next we will determine whether deregulation of this panel of miRNAs also correlates with the survival of HCC patients, and whether detecting all these miRNAs together is more precise in identifying the prognosis of HCC patients.

As current chemotherapy for HCC is not effective, biological therapy of HCC, including gene therapy and immunotherapy, has been extensively investigated. In this study, the antitumor effect of miR-199a/b-3p was determined both in vitro and in vivo, suggesting its considerable potential in HCC gene

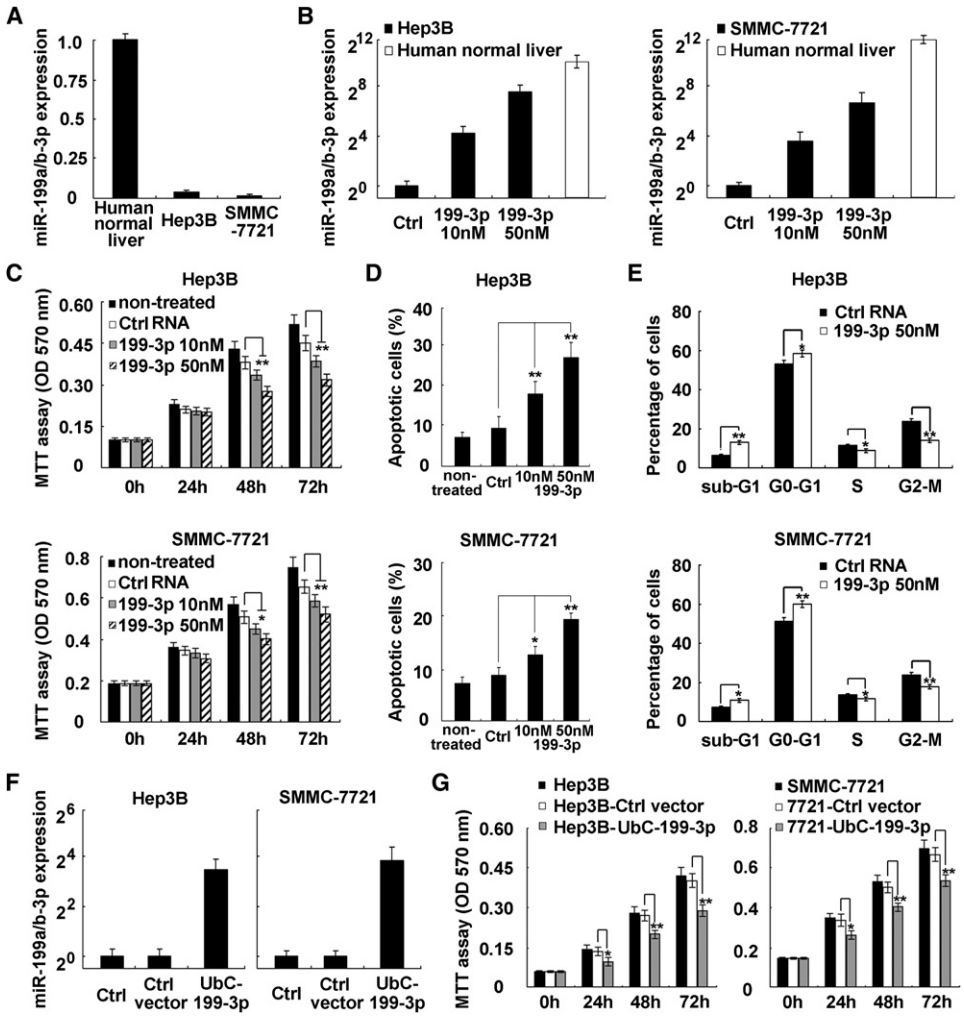

Figure 3. miR-199a/b-3p Inhibits HCC Growth In Vitro

(A) miR-199a/b-3p expression in human normal liver, Hep3B, and SMMC-7721 HCC cell lines was detected using real-time qRT-PCR.

(B) Hep3B and SMMC-7721 HCC cells were transfected with miR-199a/b-3p mimics at a final concentration of 10 or 50 nM. miR-199a/b-3p expression was detected using real-time qRT-PCR at 48 hr posttransfection. miR-199a/b-3p expression in human normal liver tissue was also shown as indicated.

(C–E) Hep3B and SMMC-7721 HCC cells were transfected as in (B). In the indicated time periods posttransfection, cell growth rate was evaluated using MTT assay (C). Cells were stained using propidium iodide (PI) and Annexin V 72 hr posttransfection and analyzed by FACS. The Annexin V-positive cells were regarded as apoptotic cells (D) and the cell cycle distribution was calculated (E).

(F and G) miR-199a/b-3p expression in Hep3B and SMMC-7721 HCC cells stably overexpressed miR-199a/b-3p was detected using real-time qRT-PCR (F). The cell growth rate of these cells was detected by MTT assay (G).

Data are shown as mean ± SD (n = 4) of one representative experiment. Similar results were obtained in three independent experiments. *, $p < 0.05$; **, $p < 0.01$. See also Figure S3.

therapy. The main obstacle for gene therapy is how to effectively and safely deliver the genes into cancer cells or tumor microenvironment. As compared with other tissues, liver tissue is easier to be targeted by both nonviral and viral delivery systems for effector molecules and genes. Here, we used both cholesterol-conjugated small RNAs and AAV8 delivery system, and confirmed that both approaches could effectively restore miR-199a/b-3p expression in HCC tissues of HCC-bearing nude mice. Cholesterol-conjugated small RNAs are easier for dose control, which are drug-like properties, but they can not sustain the restoration of small RNAs for a long time period as compared with viral delivery systems. AAV8 delivery system is promising for liver-targeted gene therapy for its vector stability, safety, and low immunogenicity, and it can sustain the gene expression for a relative long time period. As reported, enforced expression of miR-26a using AAV8 delivery system inhibited tumorigenicity in mouse HCC model, also suggesting its therapeutic potential (Kota et al., 2009). If combined with the enforced expression of other deregulated miRNAs, or even together with coding genes bearing antitumor properties, AAV8-mediated miR-199a/b-3p in vivo delivery may be more promising in gene therapy for HCC.

Molecular mechanisms contributing to HCC pathogenesis have been extensively investigated, and deregulated cell

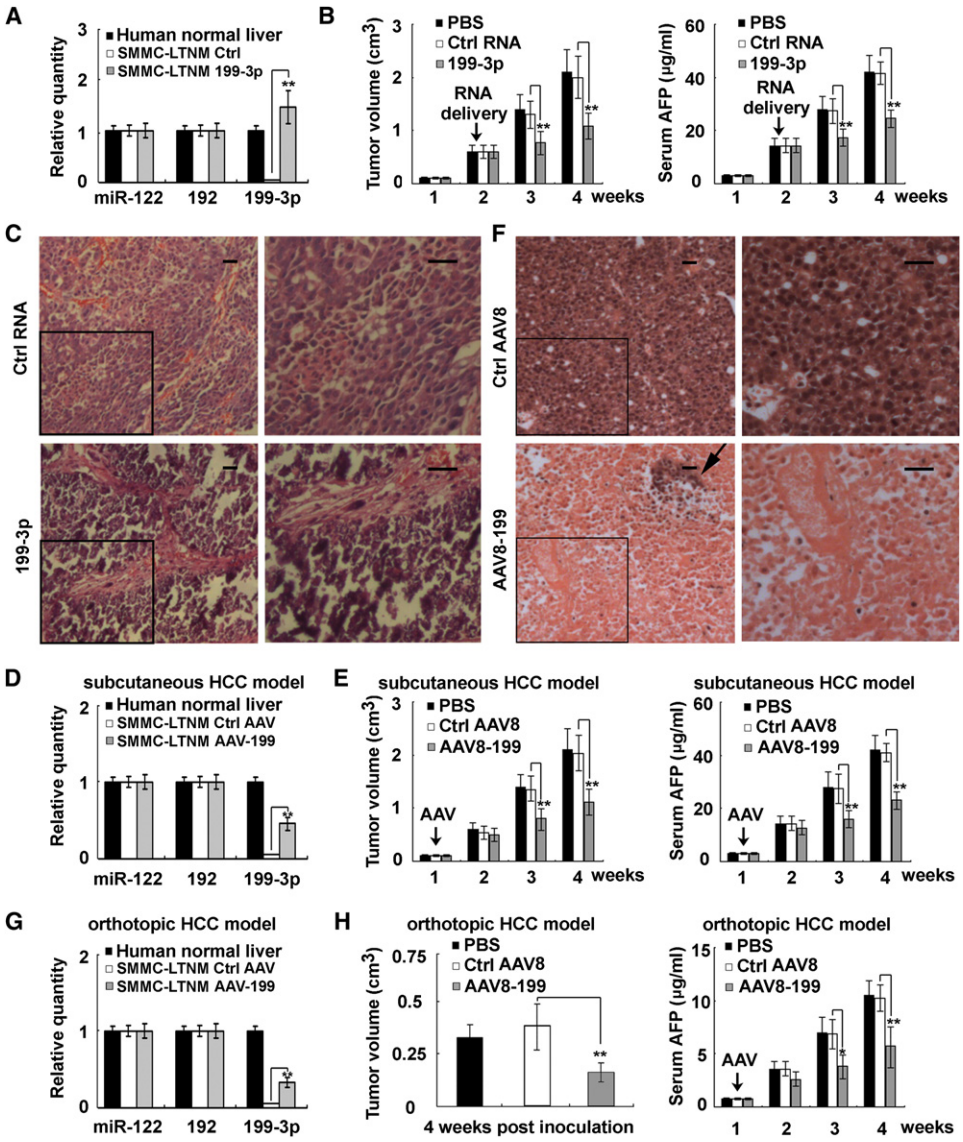

Figure 4. miR-199a/b-3p Inhibits HCC Growth In Vivo

(A) Real-time qRT-PCR analysis of miR-122, miR-192, and miR-199a/b-3p expression in human normal liver tissue, SMMC-LTNM tumor tissue 72 hr after intratumoral injection of cholesterol-conjugated miR-199a/b-3p mimics or control mimics.

(B and C) Effect of miR-199a/b-3p restoration on SMMC-LTNM tumor growth. Two weeks after subcutaneous inoculation of SMMC-LTNM tumor mass, HCC-bearing nude mice were treated by intratumoral injection of cholesterol-conjugated miR-199a/b-3p mimics. Tumor volume and serum AFP were detected as indicated in (B). H&E staining of HCC tissues was performed 2 weeks after intratumoral injection of cholesterol-conjugated miR-199a/b-3p mimics. Necrotic area in HCC tissues was shown as indicated in (C). Scale bars, 50 μm.

(D–F) Effect of AAV8-miR-199a/b-3p administration on tumor growth of subcutaneous SMMC-LTNM model. One week after subcutaneous inoculation of SMMC-LTNM tumor mass, AAV8-miR-199a/b-3p was intratumorally injected twice a week for 3 weeks. miR-122, miR-192, and miR-199a/b-3p expression in SMMC-LTNM tumor tissue was detected by qRT-PCR (D). Tumor volume and serum AFP were detected as indicated in (E). H&E staining of HCC tissues was also performed 3 weeks after AAV administration. Necrotic area and rare living tumor cell island (arrow) are shown as indicated in (F). Scale bars, 50 μm.

(G and H) One week after orthotopic inoculation of SMMC-LTNM tumor mass, AAV8-miR-199a/b-3p was delivered by a single tail vein injection of 1×10^{12} vg. miR-122, miR-192, and miR-199a/b-3p expression in orthotopic SMMC-LTNM tumor tissue was detected 3 weeks post AAV8-miR-199a/b-3p administration (G). Tumor volume 3 weeks post AAV8-miR-199a/b-3p systemic administration was measured and serum AFP was detected as indicated in (H).

Data are shown as mean ± SD (n = 4) of one representative experiment. Similar results were obtained in three independent experiments. *, $p < 0.05$; **, $p < 0.01$. See also Figure S4.

signaling pathways, including MAPK, PI3K-mTOR, and Wnt-β-Catenin pathways, have been found to play pivotal roles in HCC carcinogenesis and progression. Among them, the activated Raf/MEK/ERK signals are well-accepted prosurvival pathway in HCC. The antitumor effect of miR-199a/b-3p is determined to be mediated by inhibition of PAK4 and downstream ERK activation. Interestingly, during revision of this work, miR-199a-3p was reported to inhibit HCC cell cycle progression in vitro by

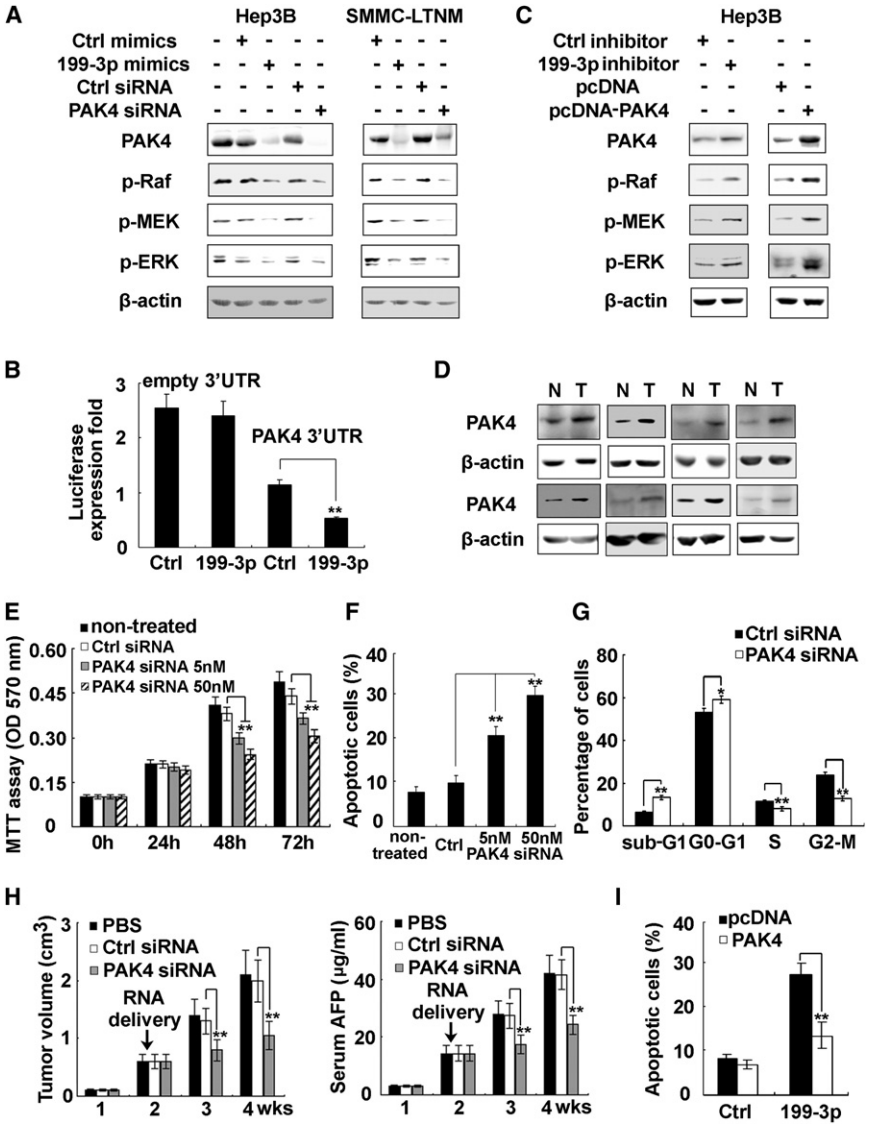

Figure 5. miR-199a/b-3p Inhibits PAK4/Raf/MEK/ERK Pathway in HCC

(A) Hep3B cells were transfected as in (3B and 5E) or HCC-bearing nude mice (SMMC-LTNM) were treated as in (4B and 5H) as indicated. Expression of β-actin (internal control), PAK4, phosphorylated Raf, MEK, and ERK were detected by western blot. Data are shown as a representative of three independent experiments.

(B) HEK293 cells were cotransfected with empty pMIR-Report firefly luciferase reporter plasmids or PAK4 3′ UTR firefly luciferase reporter plasmids, pTK-Renilla-luciferase plasmids, together with miR-199a/b-3p mimics as indicated. After 24 hr, firefly luciferase activity was measured and normalized by Renilla luciferase activity.

(C) Hep3B cells were transfected with miR-199a/b-3p inhibitor as in (3B), or PAK4 expressing plasmid as indicated. Expression of the indicated proteins was detected by western blot as in (A).

(D) Expression of PAK4 and β-actin (internal control) were detected by western blot in eight available HCC protein samples. The patient numbers were 25, 29, 32, 34, 35, 37, 39, and 40 in Table S4. N, matched nonneoplastic control; T, HCC tissue.

(E–G) Hep3B HCC cells were transfected with PAK4 siRNA as in (3B). Cell growth (E), apoptosis (F), and cell cycle (G) were detected and analyzed as in Figures 3C–3E.

(H) Effect of PAK4 knockdown on HCC tumor growth in vivo. HCC-bearing nude mice SMMC-LTNM were treated with intratumoral injection of cholesterol-conjugated PAK4 siRNA as in Figure 4B). Tumor volume and serum AFP were detected as indicated.

(I) Hep3B cells stably transfected with PAK4 expressing plasmid were transfected with miR-199a/b-3p mimics as in (3B). Cell apoptosis was detected and analyzed as in (3C).

Data are shown as mean ± SD (n = 4) of one representative experiment. Similar results were obtained in three independent experiments. *, $p < 0.05$; **, $p < 0.01$.

See also Figure S5 and Table S11.

targeting c-Met and mTOR expression (Fornari et al., 2010). Indeed, a single miRNA has been thought to target multiple mRNAs, named "targetome," to regulate gene expression (Selbach et al., 2008). In this study, c-Met and mTOR were also found to be repressed in miR-199a/b-3p overexpressed Hep3B cells. Previous reports showed that Hepatocyte growth factor (HGF) may activate downstream PAK4 via PI3K-mTOR pathway through receptor c-Met (Wells et al., 2002). Hence, major players in this pathway may be tightly regulated by miR-199a/b-3p expression in the liver, and miR-199a/b-3p restoration could target c-Met/PI3K/PAK4/ERK pathway to repress HCC progression. However, there may be other molecules or signaling pathways which are also targeted by miR-199a/b-3p, and some of them may be still unknown in HCC. This presumption may raise interesting future work to reveal the entire functions of miR-199a/b-3p in HCC carcinogenesis and progression.

The miRNomes of human normal liver, hepatitis liver, and HCC have been presented in this study, providing resources for investigating the roles of miRNAs in liver biology and liver diseases. Interestingly, no significant difference was found among the miRNomes of human normal liver, hepatitis liver, and nonneoplastic liver tissues bearing HBV or HCV infection. It does not exclude the possibility that miRNAs do not influence or participate in viral infection and hepatitis. Maybe viral infection or liver inflammation can only induce or repress the expression of some poorly expressed miRNAs, or the abundant miRNAs may also influence the replication of hepatitis virus. Moreover, whether HBV or HCV encode virus-derived miRNAs is also an important and interesting topic remaining to be investigated in these miRNomes.

EXPERIMENTAL PROCEDURES

Tissues and Cell Lines

Liver tissue samples were obtained from patients during operation, and the details were shown in Tables S3, S4, S8, and S10. For survival analysis, four independent cohorts of HCC patients from four different hospitals were

used. They are Cohort 1, 142 HCC patients from Sun Yat-sen University (Guangzhou, China); Cohort 2, 152 patients from Affiliated Tumor Hospital of Guangxi Medical University (Nanning, China); Cohort 3, 102 HCC patients from Eastern Hepatobiliary Surgery Hospital (Shanghai, China); and Cohort 4, 108 HCC patients from Zhongshan Hospital (Shanghai, China). Surgically removed tissues were quickly frozen in liquid nitrogen until analysis. Human normal liver tissues were obtained from distal normal liver tissue of liver hemangioma patients. HBV infected liver tissue and severe chronic hepatitis B liver tissue were obtained from distal liver tissue of the liver hemangioma patients with HBV infection or severe chronic hepatitis B. HCC samples and matched controls were obtained form HCC patients. All samples were collected with the informed consent of the patients and the experiments were approved by Institute Research Ethics Committee at Cancer Center, Sun Yat-sen University; ethics committee of Guangxi Medical University; ethics committee of Second Military Medical University; and Research ethics committee at Liver Cancer Institute and Zhongshan Hospital, Fudan University. HEK293, Hep3B, SMMC-7721, Huh7, and HepG2 cell lines were obtained and cultured as described previously (An et al., 2008; Wang et al., 2009c).

Illumina Solexa MPSS

Total RNA, containing miRNA, was extracted using miRNeasy Mini Kit (QIAGEN 217004, Germany) and passed the RNA quality control for Solexa sequencing. The sequencing procedure was described previously (Chen et al., 2009). Sequencing data were mainly analyzed using SOAP (Short Oligonucleotide Alignment Program) as described previously (Li et al., 2008). Clean sequenced reads (excluding reads containing ambiguous base and adaptor contaminants) (Table S1) yielded by Solexa sequencing were used for further analysis. After removal of reads classified as small RNAs from rRNA etc. (rRNA, tRNA, scRNA, snRNA, snoRNA), repeat-associated small RNAs, and mRNAs (exons/introns) (Table S1), the sequenced reads of known miRNAs and each individual of them, including small RNAs perfectly matching miRBase precursor sequence and those identified as known miRNA editing polymorphisms (Ebhardt et al., 2009; Wu et al., 2007), were annotated and calculated.

Reagents

Antibodies specific to PAK4 (3242), phospho-Raf1 (9427), and phospho-MEK (2354) were from Cell Signaling Technology (Danvers, MA). Antibodies specific to phospho-ERK, phospho-p38, phospho-JNK, β-actin, and horseradish peroxidase-coupled secondary antibodies were described previously (An et al., 2008; Hou et al., 2009; Wang et al., 2009b). Cholesterol-conjugated miR-199a/b-3p mimics and PAK4 siRNA for in vivo RNA delivery, miR-199a/b-3p mimics and inhibitors for in vitro transfection, and their respective negative controls were from Ribobio Co. (Guangzhou, China) (Li et al., 2009).

RNA Quantification

Real-time qRT-PCR assay was performed as described previously (Hou et al., 2009). For evaluating miRNA expression in each HCC tissue compared with its matched control, miRNA level in tumor sample is divided by that in matched nonneoplastic control (HCC/control). For pri-miR-199 assay, the detection kits were from Applied Biosystems (Hs03302808_pri, Hs03302922_pri, and Hs03302926_pri) (Carlsbad, CA). Other primers used were shown in Supplemental Experimental Procedures.

Bisulfate Sequencing

Genomic DNA was extracted, digested, purified, bisulfate converted and purified, PCR amplificated, cloned, and sequenced as reported (Kim et al., 2008).

ChIP Assay and Real-Time PCR

The cells were crosslinked and processed according to the Millipore (17-229) Chromatin Immunoprecipitation (ChIP) Assay Kit (Temecula, CA) protocol. Antibodies to H3K4me3 (Millipore 07-473), H3K9me3 (Millipore 05-1242), H3K27me3 (Millipore 07-449), H4K20me3 (Abcam ab9053), or control IgG (Santa Cruz sc-2027 or sc-2025) were used at 5 μg per immunoprecipitation for the specific immunoprecipitation of respective histone residues. Ten microliters sonicated but preimmunoprecipitated DNA from each sample was used as input controls. ChIP results were analyzed by real-time PCR as described previously (Hou et al., 2009). The primers spanning the reported CpG islands of miR-199a-1 and miR-199a-2 were shown in Supplemental Experimental Procedures. Final results of each sample were normalized to the inputs. Real-time PCR of GAPDH on the immunoprecipitated DNA fractions was performed as additional internal controls (Ting et al., 2005).

Transfection

Hep3B cells (2×10^5) were seeded into each well of 6-well plates and incubated overnight, and then transfected with RNAs or plasmids using INTERFERin or jetPEI (Polyplus-transfection, France), respectively, as described previously (Hou et al., 2009; Wang et al., 2009b).

In Vivo Assay

All animal experiments were undertaken in accordance with the National Institute of Health Guide for the Care and Use of Laboratory Animals, with the approval of the Scientific Investigation Board of Second Military Medical University, Shanghai. Human HCC-bearing male nude mice with subcutaneous passage of SMMC-LTNM were used for evaluating the antitumor effect of miR-199a/b-3p in vivo. For preparation of subcutaneous model, 0.2 ml grinded SMMC-LTNM tumor tissue was subcutaneously injected and inoculated. For preparation of orthotopic HCC model, 0.02 ml grinded SMMC-LTNM tumor tissue was directly injected and inoculated into the liver of nude mice whose abdomen was surgically opened. For delivery of cholesterol-conjugated RNA, 10 nmol RNA in 0.1 ml saline buffer was locally injected into the tumor mass once every 3 days for 2 weeks. The rAAV (serotype 8) vector expressing miR-199a/b-3p under promoter CAG was constructed as previously described (Han et al., 2005). For AAV8 administration, 2×10^{11} vg AAV8 in 0.05 ml saline buffer was intratumorally injected into SMMC-LTNM subcutaneous model twice a week for 3 weeks, or 1×10^{12} vg AVV8 in 0.2 ml saline buffer was injected through a single tail vein injection for SMMC-LTNM orthotopic model. Tumor size was measured as described previously (Qi et al., 2003). Serum AFP was detected using ELISA (Autobio, Zhengzhou, China).

Statistical Analysis

Data are presented as mean ± SD. Statistical comparisons between experimental groups were analyzed by Student's t test and a two-tailed $p < 0.05$ was taken to indicate statistical significance. For analyzing survival of HCC patients, log-rank test in SPSS 17.0 was used with the p values indicated. Analysis of univariate or multivariate Cox proportional hazards regression was also conducted using SPSS 17.0 with the hazard ratios and p values indicated.

For information on the following, please see Supplemental Experimental Procedures: 3′ UTR luciferase reporter assay, RNA interference, MTT assay, apoptosis assay, cell cycle analysis, western blot, and primers.

ACCESSION NUMBER

The Solexa sequencing data are available in GEO database (www.ncbi.nlm.nih.gov/geo/) with accession number GSE21279.

SUPPLEMENTAL INFORMATION

Supplemental Information includes Supplemental Experimental Procedures, five figures, and eleven tables and can be found with this article online at doi:10.1016/j.ccr.2011.01.001.

ACKNOWLEDGMENTS

We thank Ms. Mei Jin, Yan Li, Tingting Fang, and Miao Chen for technical assistance, Drs. Ning Li, Jun Wang, Jinjie Duan, and Qibin Li from BGI-Shenzhen, Drs. Yuan Xie, and Xiaoling Luo from Guangxi Medical University, and Drs. Chaofeng Han, Nan Li, Yanmei Han, Taoyong Chen, Yan Gu, Zhubo Chen, Dong Li, Feng Ma, Pin Wang, Xiaoping Su, Minggang Zhang, Xiongfei Xu, and Liang Tang from our institute for valuable discussions. This work was supported by grants from the National 115 Key Project of China (2008ZX10002-23, 2008ZX10002-008), National High-Tech Projects (2007AA021100), National Natural Science Foundation of China (30721091),

and National Key Basic Research Program of China (2007CB512403, 2009CB522402). The authors declare no competing financial interests.

Received: April 1, 2010
Revised: October 10, 2010
Accepted: December 29, 2010
Published: February 14, 2011

REFERENCES

An, H., Hou, J., Zhou, J., Zhao, W., Xu, H., Zheng, Y., Yu, Y., Liu, S., and Cao, X. (2008). Phosphatase SHP-1 promotes TLR- and RIG-I-activated production of type I interferon by inhibiting the kinase IRAK1. Nat. Immunol. *9*, 542–550.

Basso, K., Sumazin, P., Morozov, P., Schneider, C., Maute, R.L., Kitagawa, Y., Mandelbaum, J., Haddad, J., Jr., Chen, C.Z., Califano, A., et al. (2009). Identification of the human mature B cell miRNome. Immunity *30*, 744–752.

Braconi, C., and Patel, T. (2008). MicroRNA expression profiling: a molecular tool for defining the phenotype of hepatocellular tumors. Hepatology *47*, 1807–1809.

Brown, B.D., Gentner, B., Cantore, A., Colleoni, S., Amendola, M., Zingale, A., Baccarini, A., Lazzari, G., Galli, C., and Naldini, L. (2007). Endogenous microRNA can be broadly exploited to regulate transgene expression according to tissue, lineage and differentiation state. Nat. Biotechnol. *25*, 1457–1467.

Budhu, A., Jia, H.L., Forgues, M., Liu, C.G., Goldstein, D., Lam, A., Zanetti, K.A., Ye, Q.H., Qin, L.X., Croce, C.M., et al. (2008). Identification of metastasis-related microRNAs in hepatocellular carcinoma. Hepatology *47*, 897–907.

Cammarano, M.S., Nekrasova, T., Noel, B., and Minden, A. (2005). Pak4 induces premature senescence via a pathway requiring p16INK4/p19ARF and mitogen-activated protein kinase signaling. Mol. Cell. Biol. *25*, 9532–9542.

Chen, X., Li, Q., Wang, J., Guo, X., Jiang, X., Ren, Z., Weng, C., Sun, G., Wang, X., Liu, Y., et al. (2009). Identification and characterization of novel amphioxus microRNAs by Solexa sequencing. Genome Biol. *10*, R78.

Coulouarn, C., Factor, V.M., Andersen, J.B., Durkin, M.E., and Thorgeirsson, S.S. (2009). Loss of miR-122 expression in liver cancer correlates with suppression of the hepatic phenotype and gain of metastatic properties. Oncogene *28*, 3526–3536.

Ebhardt, H.A., Tsang, H.H., Dai, D.C., Liu, Y., Bostan, B., and Fahlman, R.P. (2009). Meta-analysis of small RNA-sequencing errors reveals ubiquitous post-transcriptional RNA modifications. Nucleic Acids Res. *37*, 2461–2470.

Esteller, M. (2008). Epigenetics in cancer. N. Engl. J. Med. *358*, 1148–1159.

Eswaran, J., Soundararajan, M., and Knapp, S. (2009). Targeting group II PAKs in cancer and metastasis. Cancer Metastasis Rev. *28*, 209–217.

Fornari, F., Milazzo, M., Chieco, P., Negrini, M., Calin, G.A., Grazi, G.L., Pollutri, D., Croce, C.M., Bolondi, L., and Gramantieri, L. (2010). MiR-199a-3p regulates mTOR and c-Met to influence the doxorubicin sensitivity of human hepatocarcinoma cells. Cancer Res. *70*, 5184–5193.

Gramantieri, L., Ferracin, M., Fornari, F., Veronese, A., Sabbioni, S., Liu, C.G., Calin, G.A., Giovannini, C., Ferrazzi, E., Grazi, G.L., et al. (2007). CyclinG1 is a target of miR-122a, a microRNA frequently down-regulated in human hepatocellular carcinoma. Cancer Res. *67*, 6092–6099.

Gramantieri, L., Fornari, F., Callegari, E., Sabbioni, S., Lanza, G., Croce, C.M., Bolondi, L., and Negrini, M. (2008). MicroRNA involvement in hepatocellular carcinoma. J. Cell. Mol. Med. *12*, 2189–2204.

Gramantieri, L., Fornari, F., Ferracin, M., Veronese, A., Sabbioni, S., Calin, G.A., Grazi, G.L., Croce, C.M., Bolondi, L., and Negrini, M. (2009). MicroRNA-221 targets Bmf in hepatocellular carcinoma and correlates with tumor multifocality. Clin. Cancer Res. *15*, 5073–5081.

Griffiths-Jones, S., Grocock, R.J., van Dongen, S., Bateman, A., and Enright, A.J. (2006). miRBase: microRNA sequences, targets and gene nomenclature. Nucleic Acids Res. *34*, D140–D144.

Han, G., Li, Y., Wang, J., Wang, R., Chen, G., Song, L., Xu, R., Yu, M., Wu, X., Qian, J., and Shen, B. (2005). Active tolerance induction and prevention of autoimmune diabetes by immunogene therapy using recombinant adenoassociated virus expressing glutamic acid decarboxylase 65 peptide GAD(500-585). J. Immunol. *174*, 4516–4524.

Hou, J., Wang, P., Lin, L., Liu, X., Ma, F., An, H., Wang, Z., and Cao, X. (2009). MicroRNA-146a feedback inhibits RIG-I-dependent Type I IFN production in macrophages by targeting TRAF6, IRAK1, and IRAK2. J. Immunol. *183*, 2150–2158.

Hua, Y.J., Tang, Z.Y., Tu, K., Zhu, L., Li, Y.X., Xie, L., and Xiao, H.S. (2009). Identification and target prediction of miRNAs specifically expressed in rat neural tissue. BMC Genomics *10*, 214.

Ji, J., Shi, J., Budhu, A., Yu, Z., Forgues, M., Roessler, S., Ambs, S., Chen, Y., Meltzer, P.S., Croce, C.M., et al. (2009a). MicroRNA expression, survival, and response to interferon in liver cancer. N. Engl. J. Med. *361*, 1437–1447.

Ji, J., Yamashita, T., Budhu, A., Forgues, M., Jia, H.L., Li, C., Deng, C., Wauthier, E., Reid, L.M., Ye, Q.H., et al. (2009b). Identification of microRNA-181 by genome-wide screening as a critical player in EpCAM-positive hepatic cancer stem cells. Hepatology *50*, 472–480.

Kim, S., Lee, U.J., Kim, M.N., Lee, E.J., Kim, J.Y., Lee, M.Y., Choung, S., Kim, Y.J., and Choi, Y.C. (2008). MicroRNA miR-199a* regulates the MET proto-oncogene and the downstream extracellular signal-regulated kinase 2 (ERK2). J. Biol. Chem. *283*, 18158–18166.

Kota, J., Chivukula, R.R., O'Donnell, K.A., Wentzel, E.A., Montgomery, C.L., Hwang, H.W., Chang, T.C., Vivekanandan, P., Torbenson, M., Clark, K.R., et al. (2009). Therapeutic microRNA delivery suppresses tumorigenesis in a murine liver cancer model. Cell *137*, 1005–1017.

Kutay, H., Bai, S., Datta, J., Motiwala, T., Pogribny, I., Frankel, W., Jacob, S.T., and Ghoshal, K. (2006). Downregulation of miR-122 in the rodent and human hepatocellular carcinomas. J. Cell. Biochem. *99*, 671–678.

Ladeiro, Y., Couchy, G., Balabaud, C., Bioulac-Sage, P., Pelletier, L., Rebouissou, S., and Zucman-Rossi, J. (2008). MicroRNA profiling in hepatocellular tumors is associated with clinical features and oncogene/tumor suppressor gene mutations. Hepatology *47*, 1955–1963.

Landgraf, P., Rusu, M., Sheridan, R., Sewer, A., Iovino, N., Aravin, A., Pfeffer, S., Rice, A., Kamphorst, A.O., Landthaler, M., et al. (2007). A mammalian micro-RNA expression atlas based on small RNA library sequencing. Cell *129*, 1401–1414.

Li, R., Li, Y., Kristiansen, K., and Wang, J. (2008). SOAP: short oligonucleotide alignment program. Bioinformatics *24*, 713–714.

Li, H., Xie, H., Liu, W., Hu, R., Huang, B., Tan, Y.F., Xu, K., Sheng, Z.F., Zhou, H.D., Wu, X.P., et al. (2009). A novel microRNA targeting HDAC5 regulates osteoblast differentiation in mice and contributes to primary osteoporosis in humans. J. Clin. Invest. *119*, 3666–3677.

Liu, L., Cao, Y., Chen, C., Zhang, X., McNabola, A., Wilkie, D., Wilhelm, S., Lynch, M., and Carter, C. (2006). Sorafenib blocks the RAF/MEK/ERK pathway, inhibits tumor angiogenesis, and induces tumor cell apoptosis in hepatocellular carcinoma model PLC/PRF/5. Cancer Res. *66*, 11851–11858.

McCarty, D.M. (2008). Self-complementary AAV vectors; advances and applications. Mol. Ther. *16*, 1648–1656.

Murakami, Y., Yasuda, T., Saigo, K., Urashima, T., Toyoda, H., Okanoue, T., and Shimotohno, K. (2006). Comprehensive analysis of microRNA expression patterns in hepatocellular carcinoma and non-tumorous tissues. Oncogene *25*, 2537–2545.

Qi, R., An, H., Yu, Y., Zhang, M., Liu, S., Xu, H., Guo, Z., Cheng, T., and Cao, X. (2003). Notch1 signaling inhibits growth of human hepatocellular carcinoma through induction of cell cycle arrest and apoptosis. Cancer Res. *63*, 8323–8329.

Sarasin-Filipowicz, M., Krol, J., Markiewicz, I., Heim, M.H., and Filipowicz, W. (2009). Decreased levels of microRNA miR-122 in individuals with hepatitis C responding poorly to interferon therapy. Nat. Med. *15*, 31–33.

Selbach, M., Schwanhäusser, B., Thierfelder, N., Fang, Z., Khanin, R., and Rajewsky, N. (2008). Widespread changes in protein synthesis induced by microRNAs. Nature *455*, 58–63.

Tao, W.Z., Xu, B., Gong, Z.J., and Ni, C.R. (2007). Pathological changes of human hepatocellular carcinoma after continuous passaging in nude mice. Chin. J. Cancer Biother. *14*, 163–168.

Tao, W.Z., Zheng, W.Q., and Gong, Z.J. (1998). The tumor invasion and metastasis in the transplantation of transplanted human hepatocellular carcinoma into nude mice abdominal cavity and orthotopic hepatic tissue. Dier Junyi Daxue Xuebao. *19*, 54–56.

Ting, A.H., Schuebel, K.E., Herman, J.G., and Baylin, S.B. (2005). Short double-stranded RNA induces transcriptional gene silencing in human cancer cells in the absence of DNA methylation. Nat. Genet. *37*, 906–910.

Ura, S., Honda, M., Yamashita, T., Ueda, T., Takatori, H., Nishino, R., Sunakozaka, H., Sakai, Y., Horimoto, K., and Kaneko, S. (2009). Differential microRNA expression between hepatitis B and hepatitis C leading disease progression to hepatocellular carcinoma. Hepatology *49*, 1098–1112.

Varnholt, H., Drebber, U., Schulze, F., Wedemeyer, I., Schirmacher, P., Dienes, H.P., and Odenthal, M. (2008). MicroRNA gene expression profile of hepatitis C virus-associated hepatocellular carcinoma. Hepatology *47*, 1223–1232.

Wang, B., Majumder, S., Nuovo, G., Kutay, H., Volinia, S., Patel, T., Schmittgen, T.D., Croce, C., Ghoshal, K., and Jacob, S.T. (2009a). Role of microRNA-155 at early stages of hepatocarcinogenesis induced by choline-deficient and amino acid-defined diet in C57BL/6 mice. Hepatology *50*, 1152–1161.

Wang, C., Chen, T., Zhang, J., Yang, M., Li, N., Xu, X., and Cao, X. (2009b). The E3 ubiquitin ligase Nrdp1 'preferentially' promotes TLR-mediated production of type I interferon. Nat. Immunol. *10*, 744–752.

Wang, C., Qi, R., Li, N., Wang, Z., An, H., Zhang, Q., Yu, Y., and Cao, X. (2009c). Notch1 signaling sensitizes tumor necrosis factor-related apoptosis-inducing ligand-induced apoptosis in human hepatocellular carcinoma cells by inhibiting Akt/Hdm2-mediated p53 degradation and up-regulating p53-dependent DR5 expression. J. Biol. Chem. *284*, 16183–16190.

Wang, Y., Lee, A.T., Ma, J.Z., Wang, J., Ren, J., Yang, Y., Tantoso, E., Li, K.B., Ooi, L.L., Tan, P., et al. (2008). Profiling microRNA expression in hepatocellular carcinoma reveals microRNA-224 up-regulation and apoptosis inhibitor-5 as a microRNA-224-specific target. J. Biol. Chem. *283*, 13205–13215.

Wells, C.M., Abo, A., and Ridley, A.J. (2002). PAK4 is activated via PI3K in HGF-stimulated epithelial cells. J. Cell Sci. *115*, 3947–3956.

Wolfrum, C., Shi, S., Jayaprakash, K.N., Jayaraman, M., Wang, G., Pandey, R.K., Rajeev, K.G., Nakayama, T., Charrise, K., Ndungo, E.M., et al. (2007). Mechanisms and optimization of in vivo delivery of lipophilic siRNAs. Nat. Biotechnol. *25*, 1149–1157.

Wong, Q.W., Lung, R.W., Law, P.T., Lai, P.B., Chan, K.Y., To, K.F., and Wong, N. (2008). MicroRNA-223 is commonly repressed in hepatocellular carcinoma and potentiates expression of Stathmin1. Gastroenterology *135*, 257–269.

Wu, H., Neilson, J.R., Kumar, P., Manocha, M., Shankar, P., Sharp, P.A., and Manjunath, N. (2007). miRNA profiling of naïve, effector and memory CD8 T cells. PLoS ONE *2*, e1020.

Xiong, Y., Fang, J.H., Yun, J.P., Yang, J., Zhang, Y., Jia, W.H., and Zhuang, S.M. (2010). Effects of microRNA-29 on apoptosis, tumorigenicity, and prognosis of hepatocellular carcinoma. Hepatology *51*, 836–845.